Hindawi
Geofluids
Volume 2023, Article ID 7897165, 11 pages
https://doi.org/10.1155/2023/7897165

Research Article

Experimental Study for the Effects of Different Factors on the Sand-Carrying Capacity of Slickwater

Huan Peng,[1,2] **Wenzhe Li**,[1,2] **Juncheng Liu**,[3] **Junliang Peng**,[1,2] **Huifen Han**,[1,2] **Jiayi Liu**,[4] **Dan Liu**,[1] **and Zhifan Yang**[1,2]

[1]*Engineering Technology Research Institute of Southwest Oil & Gas Field Company, PetroChina, Chengdu 610017, China*
[2]*Key Laboratory of Shale Gas Evaluation and Exploitation of Sichuan Province, Chengdu 610017, China*
[3]*Development Division of Southwest Oil & Gas Field Company, PetroChina, Chengdu 610051, China*
[4]*Shunan Gas Field of Southwest Oil & Gas Field Company, PetroChina, Luzhou 646000, China*

Correspondence should be addressed to Huan Peng; 282600120@qq.com

Received 6 December 2022; Revised 2 January 2023; Accepted 22 March 2023; Published 4 April 2023

Academic Editor: Daoyi Zhu

With the continuous exploration and development of unconventional oil and gas reservoirs, volume fracturing technology becomes one of the necessary measures for developing shale gas and tight sandstone gas reservoirs effectively. Volume fracturing technology usually uses slickwater and drag-reducing agent as the core of the fracturing system. The composition of the fracturing system is the main factor determining its performance. Polyacrylamide has many amide groups in its main chain, high activity, and controllable performance, often in solid powder and liquid emulsion states. Furthermore, polyacrylamide which is the water-soluble drag-reducing agent is most widely used in applying current shale gas slickwater fracturing operations. Due to the low viscosity and poor sand-carrying capacity of slickwater, proppant easily settles at the bottom of hydraulic fractures. This phenomenon influences the stimulation effect of volume fracturing. Therefore, the law of sand carrying and placement of proppant in hydraulic fractures in volume fracturing plays an essential role in determining the success of the stimulation effect of volume fracturing. Through the visualization device of proppant transport in the fracture, the settlement of proppant in the fracture was studied experimentally. And through experimental equipment, the effects of different operation pumping rates, liquid viscosity, proppant type, and proppant pumping schedule on the stimulation effect were studied. The experimental results can provide strong support for volume fracturing into well material optimization and operation parameter optimization for unconventional oil and gas reservoirs.

1. Introduction

With the continuous exploration and development of unconventional oil and gas reservoirs, hydraulic fracturing has become one of the necessary measures for increasing the production of low-permeability and extra-low-permeability reservoirs [1–3]. Reservoir stimulation of shale and tight sandstone by the combination of volume fracturing, segmented multicluster perforation, and high pumping rate and the large amount of fracturing fluid usage, slickwater, and temporary plugging agent techniques can provide communication between natural fractures and rock stratigraphy. Furthermore, by communicating between natural fractures and rock laminae, the hydraulic fractures are interwoven with multilevel secondary fractures to form a fracture network system [4–7]. The fracture network system can "break up" the effective reservoir where seepage can take place, maximize the contact area between the fractures and the reservoir, and increase the volume of the reservoir stimulation as much as possible. It enables the shortest percolation distance of oil and gas from the matrix in any direction to the fracture; dramatically improves the overall permeability of the reservoir; realizes a comprehensive transformation of the reservoir in the three-dimensional direction of length, width, and height; increases the percolation area and inflow capacity; and improves the initial production and final recovery [8–13].

Due to the low viscosity of slickwater, the capacity for sand carrying is poor, so it is necessary to improve the sand-carrying capacity of fracturing fluid by increasing the injection rate of slickwater [14, 15]. However, the friction resistance in the pipeline is increased by this measure. As such, the drag-reducing agent becomes the core of slickwater fracturing technology and plays a decisive role. Furthermore, the drag-reducing agent has become a research hotspot all around the world. Polyacrylamide is a synthetic polymer obtained by the copolymerization of acrylamide and other monomers, including cationic, anionic, nonionic, and amphoteric polyacrylamide. Polyacrylamide that can be dissolved in water in any proportion is a long-chain macromolecule, and it has good thermal stability and drag reduction performance. Polyacrylamide has a large number of amide groups in the main chain, with high activity and controllable performance, usually in the state of solid powder and liquid. And polyacrylamide is the most widely used water-soluble dampening agent in shale gas slickwater fracturing operation [16, 17].

In shale gas and tight sandstone fracturing, due to the low viscosity of slickwater, poor sand-carrying capacity, and fast settling rate of proppant, the exorbitant concentration of proppant during operation is likely to cause sand plugging [18, 19]. However, the low concentration of proppant will reduce the concentration of sand laid in the fractures and the effects of fracturing stimulation. Due to the development of microfractures in the reservoir, fracturing will induce a large amount of slickwater filtration loss. And the slickwater filtration loss exacerbates the difficulty of proppant transport. As the height of the sand dike increases, the slickwater overflow area in the fracture decreases, and the liquid flow rate gradually increases. When the fluid flow rate increases to the extent that the proppant can reach dynamic suspension, the height of the sand dike is the equilibrium height. There is no proppant filling at the top of the fracture above the equilibrium height at this time. The proppant often settles at the bottom of the fracture, while there is no proppant placement in the upper part of the fracture and away from the wellbore end. This situation reduces the fracture inflow capacity and effects of fracturing stimulation. Therefore, studying the law of proppant carrying, transport, settling, and placement pattern in the fracture is crucial. The placement of proppant in the hydraulic fracturing process is essential to the outcome of the fracturing operation. The prediction of proppant placement is also the key to the design and evaluation of hydraulic fracturing [20–23].

In recent years, the studies of the sand-carrying capacity of slickwater were mainly based on laboratory experiments and numerical simulations. In the experimental studies, Liu et al. [24], Wu and Sharma [25], Hu et al. [26], and other researchers carry out experimental studies under different conditions of fracture width, pumping rate, and particle size. Through the experimental studies, they obtain the accumulation process of sand settlement and the various patterns of equilibrium height. Furthermore, they derived the empirical equations of equilibrium height, equilibrium velocity, and other characteristic parameters. In the field of numerical simulation, Olaleye et al. [27], Akhshik and Rajabi [28], Suri et al. [29], and Guo et al. [30] used the CFD method to simulate the transport process of proppant settlement in different fractures. Zhang et al. [31] use a coupled CFD-DEM method to establish a solid-liquid mixing model between parallel plates to analyze the microscopic sand-carrying mechanism of fracturing fluid in hydraulic fracturing. In general, the researches on the law of the carry and transport of proppant during the fracturing process were mainly theoretical. Field operation is often based on experience or software simulations, and there are few systematic experimental studies [32, 33]. The rheology of the liquid, flow rate, concentration, and density of proppant affect the sand-carrying capacity of slickwater, which is not conducive to grasping the laws of proppant placement, roll-up, and sand settlement distribution during sand addition [34–37]. Thus, it is necessary to carry out systematic research and analysis to compare and select fracturing fluid and proppant parameters and optimize fracturing operation parameters to ensure the formation of effective proppant placement and improve fracture conductivity [38–40].

In this paper, the proppant transport visualization device is used to observe the flow status of the sand-carrying fluid in the fracture, the scouring and carrying performance of the fluid on the proppant, and the proppant transport and settlement status through the transparent glass. By changing parameters such as pumping rate, fluid viscosity, proppant type, and pumping schedule, experimental research on the law of sand carrying and settlement in proppant-supported fracture was carried out. And the effects of different factors in volume fracturing on the sand-carrying capacity of slickwater and the settlement pattern of proppant were studied by quantitative analysis of experimental results. The research results can provide strong technical support for the preferential selection of volume fracturing entry materials and optimization of operation parameters for unconventional oil and gas reservoirs.

2. Experimental Methods

2.1. Experimental Materials. The slickwater system is commonly used in volume fracturing, and the slickwater system is formed by compounding additives such as drag-reducing agent, clay stabilizers, and drainage aids. The basic formula of our configured slickwater system is water + 0.1 ~ 0.5% emulsion drag − reducing agent + 0.25% clay stabilizer + 0.1% drainage aid. Slickwater with different viscosity values can be obtained by varying the amount of drag-reducing agent. We adopted the evaluation method for the performance of slickwater fracturing fluid which refers to the requirements and technical indexes in industry-related standards of China such as SY/T 5107-2016 (Performance Evaluation Method of Water-based Fracturing Fluid), SY/T 5613-2000 (Test Method of Physical and Chemical Properties of Mud Shale), NB/T 14003.1-2015 (Slickwater Fracturing Fluid Part 1: Performance Index and Evaluation Method), and other industry-related standards and technical indexes for the evaluation method of slickwater fracturing fluid performance. According to the standard, we conducted indoor testing to evaluate the performance of the slickwater fracturing fluid

Table 1: Performance parameters of slickwater.

Term	Apparent viscosity (mPa·s)	pH	Surface tension (mN/m)	Interfacial tension (mN/m)
Parameters	1~100	6.5~7.0	24~26	0.8~1.8
Term	CST ratio	Linear expansion rate (%)	Residue content (mg/L)	Resistance reduction rate (%)
Parameters	0.7~1.2	1.1~2.5	20~50	50~74

Table 2: 40/70 mesh ceramsite proppant performance parameters.

Term	Average diameter (μm)	Sphericity	Acid solubility (%)	Turbidity (FTU)
Parameters	320~370	0.9	3.1~6.4	38~79
Term	Bulk density (g/cm^3)	Apparent density (g/cm^3)	9% crushing grade of domestic proppant (K)	
Parameters	1.5~1.8	2.5~2.9	12.5~15.0	

system. The evaluation indexes mainly include apparent performance, resistance reduction rate, surface tension, and linear expansion rate, and the performance parameters of slickwater are shown in Table 1.

We selected the ceramsite proppant that is commonly used in current volume fracturing. According to the SY/T 5108-2014 (Test Method of Proppant Performance for Hydraulic Fracturing and Gravel Filling Operations), the basic properties of proppant such as density, roundness, turbidity, acid solubility, and anticrushing rate are evaluated. The performance parameters of the support agent are shown in Table 2. Figure 1 shows the 40/70 mesh ceramsite proppant appearance.

2.2. Experimental Device. Figures 2 and 3 show the technological process of the experimental device for visualization of the flow state in proppant-supported fracture. The experimental device comprises six parts: fluid supply and pumping system, sand mixing system, powder delivery system, visible fracture system, fluid recovery system, data acquisition, and control system. Among these six parts, the width and height of the visible fracture system are 6 mm and 0.6 m. The length of the visible fracture system is available in three modes, 2 m, 4 m, and 6 m. The maximum pumping rate of the power delivery system is 200 L/min, which can complete the engineering simulation experiment of the settlement pattern in the volume fracturing proppant-supported fracture.

The device can simulate a segment of artificial fracture in volume fracturing, which can be injected into the visual fracture system at different velocities by a powered delivery system. The flow of fracturing fluid or sand-carrying fluid in the fracture and the proppant transport and placement can be clearly observed through the transparent Plexiglas of the visual fracture system.

2.3. Experimental Steps. The experimental schedule for the visualization of the flow state in the proppant-supported fracture is as follows:

Step 1: connect the experimental apparatus, ensure the sealing of the experimental device, start the data acquisition and control system of the experimental device, and clear the data to zero.

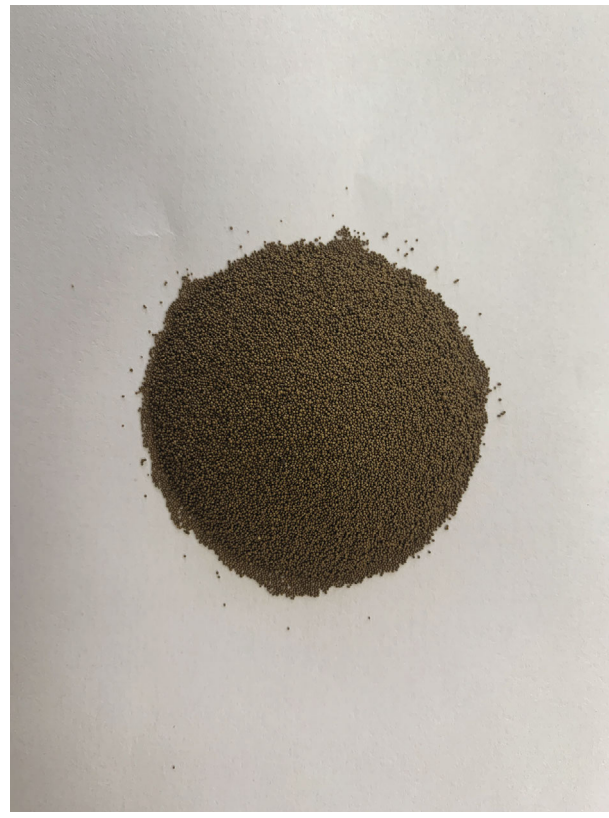

Figure 1: 40/70 mesh ceramsite proppant appearance.

Step 2: close the outlet of the sand mixing tank of the sand mixing system, inject the amount of fracturing fluid required for the experiment, calculate and measure the number of additives required for the slickwater, open the agitator of the sand mixing tank, and add the required additives.

Step 3: open the outlet of the sand mixing tank, start the screw pump of the fluid supply and pumping system, inject fracturing fluid into the simulated fracture, and wait for the fracturing fluid to fill the whole fracture.

Step 4: calculate and measure the number of proppant particles required for the experiment, add it to the powder delivery system, adjust the transfer velocity of the sand

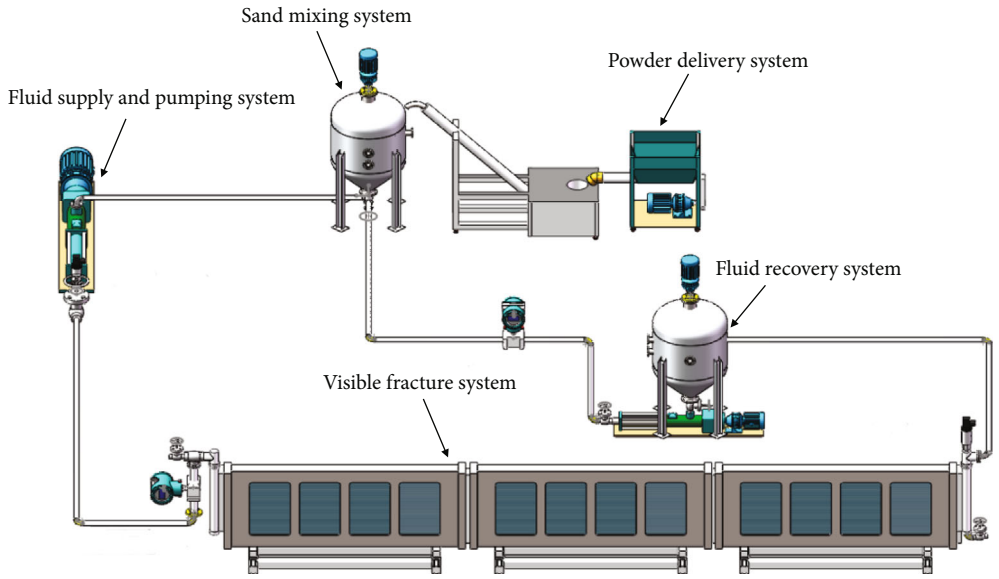

Figure 2: The technological process of an experimental device for visualization of flow state in proppant-supported fracture.

Figure 3: Experimental device for visualization of proppant flow state in proppant-supported fracture.

transfer device to ensure that it is mixed with the fracturing fluid in the sand mixing tank to reach dynamic equilibrium, adjust it to the sand concentration required for the experiment, turn on the screw pump and data acquisition system, and start the experiment.

Step 5: from the time the proppant starts to enter the fracture timing, the experimental process is filmed using the high-resolution video camera in the data acquisition and control system to record the proppant in proppant-supported fracture settlement patterns throughout the experimental process under different experimental conditions.

Step 6: after the sand mixing liquid is pumped, sand mixing system, fluid supply and pumping system, and powder delivery system are shut down, the data acquisition system is closed, and the experiment is finished.

Step 7: the visible fracture system is flushed with clean water. In the fluid recovery system, the proppant and fracturing fluid are separated and the proppant particles are collected and dried for reuse, while the fracturing fluid is uniformly recycled for disposal.

2.4. Experimental Scheme. The experiments follow the Reynolds similarity principle by converting the volume fracturing field operation pumping rate to the flow rate of the intrafracture fluid in the visible fracture system in the experimental setup, calculated as follows:

$$v_e = \frac{v_f}{h_f \times w_f \times 2} \times (h_e \times w_e). \quad (1)$$

The parameters in Equation (1) are shown in Table 3.

At present, the characteristics of the volume fracturing process are the high pumping rate, large amount of fracturing fluid and proppant usage, small particle size, and low sand ratio. The main technical parameters are as follows: the horizontal section is 1000~1500 m long, divided into 15~20 segments, each segment is divided into 4~6 clusters of perforation, the spacing of the cluster of perforation is 20~30 m, the pumping rate is 10 m^3/min or more, the average sand ratio concentration is 100~240 kg/m^3, the fracturing fluid volume is 1500~2000 m^3 per segment, and the proppant volume is 100~150 t per segment. The fracturing fluid system combines slickwater and linear rubber, and the proppant volume is mainly 40/70 mesh.

In order to study the effects of pumping rate, fluid viscosity, proppant density, and proppant pumping schedule on the law of proppant settlement, we combined the current field volume fracturing operation parameters to design experiment cases, such as in Table 4.

3. The Characteristics of Sand Carrying by Slickwater

Figure 4 indicates the transport process of proppant in fracture, where Ho is defined as the fracture height and He is defined as the equilibrium height of the sand dike. After the proppant particles enter the fracture, the sand dike will

Table 3: Meaning of the symbols in Equation (1).

Symbol	V_e	V_f	h_f
Meaning	Pumping rate of indoor experiment (m^3/min)	Field pumping rate (m^3/min)	The height of the hydraulic fracture (m)
Symbol	W_f	H_e	W_e
Meaning	The width of the hydraulic fracture (mm)	The height of fracture in visible fracture system (m)	The width of the fracture in the visible fracture system (mm)

Table 4: Experimental scheme of proppant settlement and transport in proppant-supported fracture of volumetric fracturing proppant.

No.	Pumping rate (L/min)	Liquid viscosity (mPa·s)	Proppant bulk density (g/cm^3)	Proppant concentration (kg/m^3)	Proppant pumping schedule
1	40	3	1.50	150	Sand uniformly throughout the whole process
2	60	3	1.50	150	Sand uniformly throughout the whole process
3	80	3	1.50	150	Sand uniformly throughout the whole process
4	80	30	1.50	150	Sand uniformly throughout the whole process
5	80	100	1.50	150	Sand uniformly throughout the whole process
6	60	3	1.65	150	Sand uniformly throughout the whole process
7	60	3	1.80	150	Sand uniformly throughout the whole process
8	60	3	1.50	80~220	Slope sand throughout the whole process
9	60	3	1.50	80~220	Slug slope sand throughout the whole process

gradually accumulate with time. Until the height of the sand dike no longer increases, it is the equilibrium height. The t_1~t_8 are the sand dike forms under the nth minute.

It was found that in the first to fourth minutes of the initial stage of sand carrying by slickwater, the sand-carrying liquid flows out from the borehole at high velocity. The proppant settles to the bottom of the fracture by gravity to form a sand dike. With the sand-carrying liquid's continuous pumping, the length and height of the sand dike gradually increase. Finally, the sand dike gradually reaches the equilibrium height near the fracture inlet. After reaching equilibrium height, proppant particles rolled up and sunk in the fracture reach equilibrium, and the height of the sand dike remains unchanged. This stage is sand dike formation.

In the intermediate stage of sand carrying by slickwater at 5-6 minutes, the gap between the top of the sand dike and the top of the fracture will reduce to a minimum when the sand dike near the wellbore reaches the equilibrium height. Because the number of proppant particles settling at this location equals the number of proppant being carried away, settlement occurs after the proppant is transported to the sand dike to reach the equilibrium height. Due to the injected sand-carrying liquid, the dike of sand that has reached equilibrium height flows over it and settles before flowing to a location where it has not yet reached equilibrium height. Thus, the final equilibrium height will keep moving towards the flow direction towards the front of the flow. This stage is sand dike balance.

At 7-8 minutes of the final stage of sand carrying by slickwater, the front section of the sand dike reaches the equilibrium height. In this stage, the sand dike grows only in the length direction with the injection of sand-carrying liquid, and the height always maintains the equilibrium height, and the sand dike always grows forward with the equilibrium height. This stage is sand dike advancement.

In summary, the whole process of sand carrying by slickwater and proppant settlement in fractures can be divided into three stages: sand dike formation, sand dike balance, and sand dike advancement.

4. Experimental Results and Analysis

4.1. The Effect of Pumping Rate on the Law of Sand Carrying by Slickwater. Volume fracturing with large fluid volumes and a high pumping rate is usually used to stimulate the shale gas and tight gas reservoirs. Under the condition of the same total proppant dose and concentration of proppant, we studied the effect of pumping rate on the law of sand carrying by slickwater. The pumping rates in the experimental cases are 40 L/min, 60 L/min, and 80 L/min. These three cases correspond to field operation pumping rates of 6 m^3/min, 8 m^3/min, and 12 m^3/min, respectively. The height of the sand dike with different pumping rates at different times is shown in Figure 5, and the final shape of the sand dike is shown in Figure 6.

From Figures 5 and 6, we can see that different pumping rates have a significant effect on the shape of the sand dike under the condition. As the pumping rate increases, the horizontal transport velocity of particles increases, and the equilibrium height of the sand dike decreases. The equilibrium height of the sand dike is 0.44 m when the pumping rate is 40 L/min, 0.42 m when it is 60 L/min, and 0.39 m when it is 80 L/min. The pumping rate increases cause the sand dike

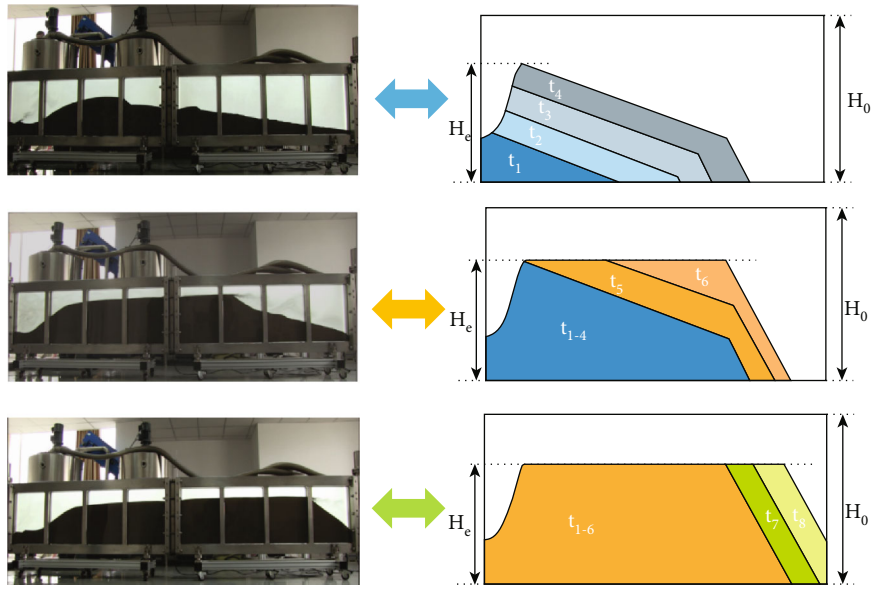

Figure 4: The process of sand carrying by slickwater and proppant transport.

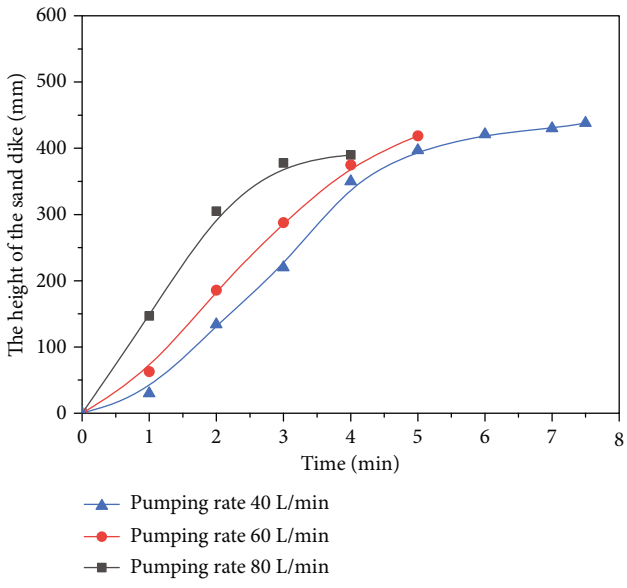

Figure 5: The height of the sand dike in sand carrying by slickwater with different pumping rates.

to become gentle and tend to transport deep into the fracture. Thus, the proppant cannot be delivered deep into the fracture when the pumping rate is low. During the process of field operation, to form a long and effective proppant-supported fracture, the operation pumping rate should be increased as much as the conditions allow. However, we cannot increase the pumping rate without limitation because the pumping rate increase causes equilibrium height reduction and low concentration of proppant near the fracture inlet. This is not conducive to forming proppant-supported fracture with high conductivity at the fracture inlet, as shown in Figure 6.

4.2. The Effect of Liquid Viscosity on the Law of Sand Carrying by Slickwater. The advantages of low viscous slickwater are low reservoir damage, large stimulation reservoir volume, and low cost, but the disadvantage is limited sand-carrying capacity. The high-viscosity fracturing fluid has a positive sand-carrying capacity, but it is harmful to the reservoir and too expensive. To improve the sand-carrying capacity of slickwater and reduce reservoir damage and the cost of volume fracturing, we need to establish a variable-viscosity slickwater liquid system. Thus, we investigated the effect of liquid viscosity on the law of proppant settlement in slickwater. The results of this part of the study can guide the optimal formation of a variable-viscosity slickwater liquid system to meet the requirements of increasing the volume of reservoir stimulation and sand-carrying capacity of slickwater. The cases used in the experiments were all performed under the same total proppant and pumping rate conditions. The pumping rate in the experiment is 80 L/min. Figure 7 reveals the height of the sand dike at different times with different liquid viscosities, and Figure 8 shows the final shape of the sand dike. It can be seen in Figure 7 that the viscosity is 3 mPa·s, 30 mPa·s, and 100 mPa·s, respectively, when the liquid is low-viscosity slickwater, medium-viscosity slickwater, and high-viscosity slickwater. The time to reach equilibrium height for sand dikes with low viscous slickwater and medium viscous slickwater was 4.0 min and 3.0 min, respectively. The equilibrium heights of sand dikes are 0.41 m and 0.32 m for low viscous slickwater (viscosity of 3 mPa·s) and medium viscous slickwater (30 mPa·s) conditions, respectively, as shown in Figure 8. Due to the high viscous slickwater with high sand-carrying capacity, the proppant advances uniformly forward in the fracture, and the settlement rate is slow. The sand dike advances uniformly in the fracture.

In summary, the effect of slickwater viscosity on the law of sand-carrying capacity by slickwater is consistent with the

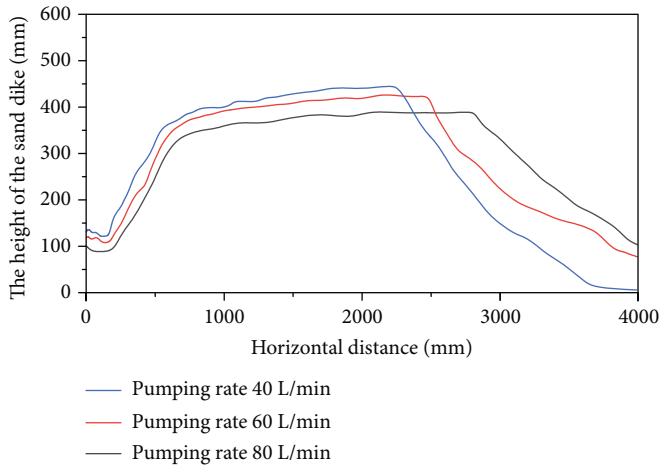

Figure 6: The shape of the sand dike formed by proppant sedimentation in sand carrying by slickwater with different pumping rates.

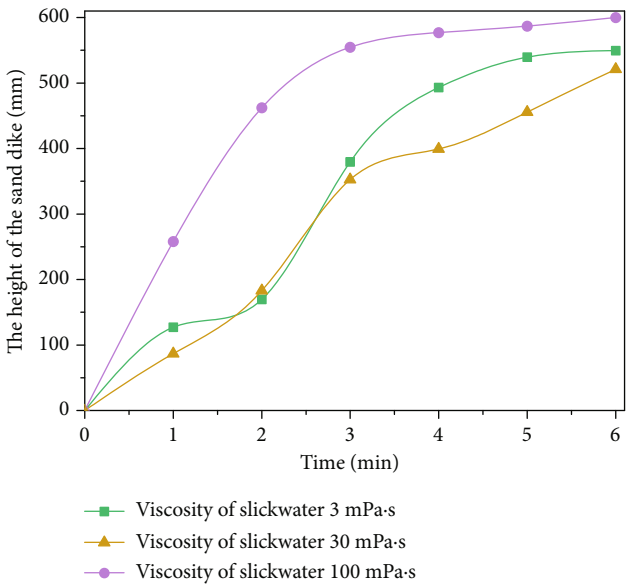

Figure 7: The height of the sand dike in sand carrying by slickwater with different liquid viscosities.

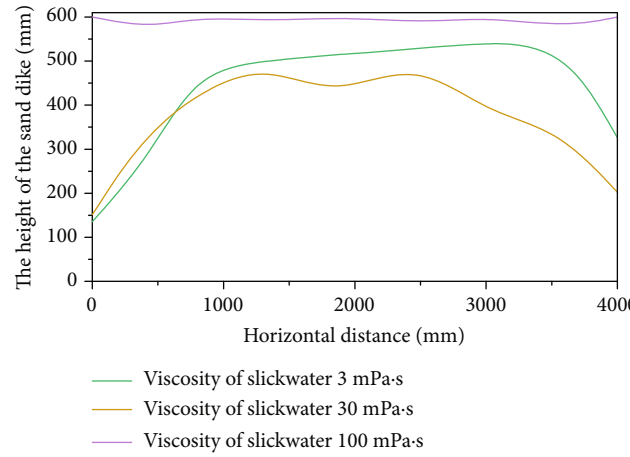

Figure 8: The shape of the sand dike formed by proppant sedimentation in sand carrying by slickwater with different liquid viscosities.

trend of pumping rate on the law of sand carrying by slickwater. Furthermore, the effect of liquid viscosity on the sand-carrying capacity of slickwater is more significant than the pumping rate. Therefore, during field operation in order to form the proppant-supported fracture with a longer length and higher conductivity, slickwater with high viscosity should be selected as far as possible under the condition of satisfying the reservoir damage so that the proppant can be transported to the fracture tips.

4.3. The Effect of Proppant Bulk Density on the Law of Sand Carrying by Slickwater. Proppant is used in volume fracturing to establish proppant-supported fracture with high conductivity, thus ensuring the reservoir stimulation effect. Under the condition of the same total proppant dose and pumping rate, the study on the effect of different proppant types on the settlement pattern of proppant was carried out, which adopts the pumping rate was 60 L/min. Figure 9 indicates the height of the sand dike at different times with different proppant densities, and the final shape of the sand dike is shown in Figure 10. It was found that different proppant density impacts the shape of the sand dike at the same total proppant dose and pumping rate. As the proppant density decreases, the horizontal transport velocity of particles decreases, and the equilibrium height of the sand dike decreases. When the proppant density is 1.80 g/cm^3, the sand dike equilibrium height is 450 mm. When the proppant density is 1.65 g/cm^3, the sand dike equilibrium height is 0.43 m. When the proppant density is 1.50 g/cm^3, the sand dike equilibrium height is 0.42 m. Sand dike thus becomes smoother, and similar to the increased pumping rate, there is a tendency for proppant to be transported deeper into the fractures. Overall, the influence of proppant density on proppant settling law is opposite to the influence of

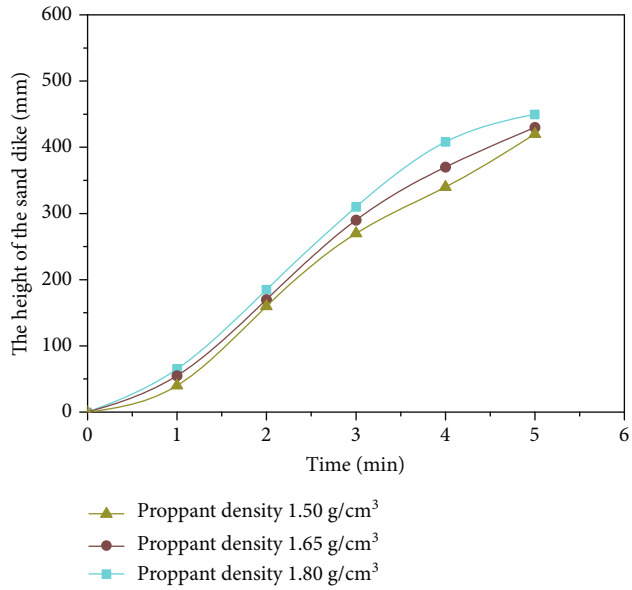

Figure 9: The height of the sand dike in sand carrying by slickwater with different proppant densities.

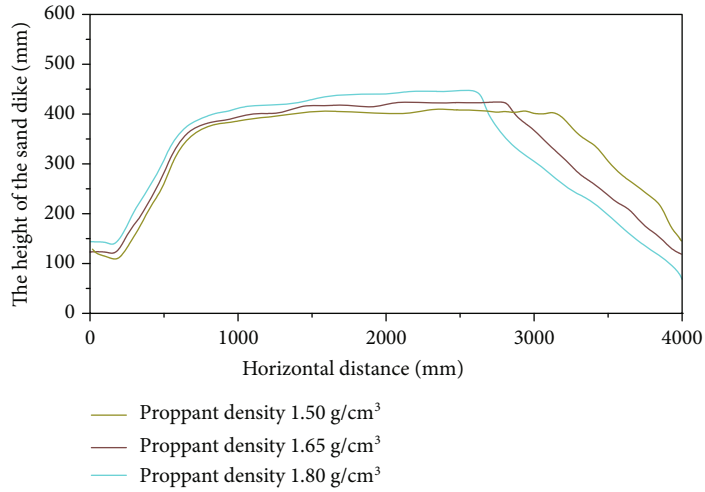

Figure 10: The shape of the sand dike formed by proppant sedimentation in sand carrying by slickwater with different proppant densities.

pumping rate on proppant settling law, and the influence of proppant density on proppant settling law is smaller than the influence of pumping rate on proppant settling law. During the field construction, to form the proppant-supported fracture with a longer length and higher conductivity, low-density proppant should be used as much as possible under the condition that the compressive strength of the proppant is satisfied, which can make the proppant delivered to the depth of the fractures.

4.4. The Effect of Proppant Pumping Schedule on the Law of Proppant Settlement. In order to meet the needs of the reservoir stimulation, slope sand and slug slope sand pumps are selected to inject the proppant schedule [13, 14]. Thus, we researched the effect of the proppant pumping schedule on the law of proppant settlement with the condition of the same total proppant dose and pumping rate, and the pumping rate in the experiment was 60 L/min. Figure 11 shows the height of the sand dike at different times with different proppant pumping schedules, and the final shape of the sand dike is shown in Figure 12. Different proppant pumping schedules significantly affect sand dike morphology for the same total proppant dose and pumping rate. The height of the sand dike grows more rapidly in uniform sand addition throughout the whole process. When slope sand addition is used, the initial increase in the height of the sand dike is slow due to the low proppant concentration at the beginning of pumping. With slope sand addition, the proppant concentration becomes more significant at the later stage of pumping, resulting in an increase in proppant concentration at the

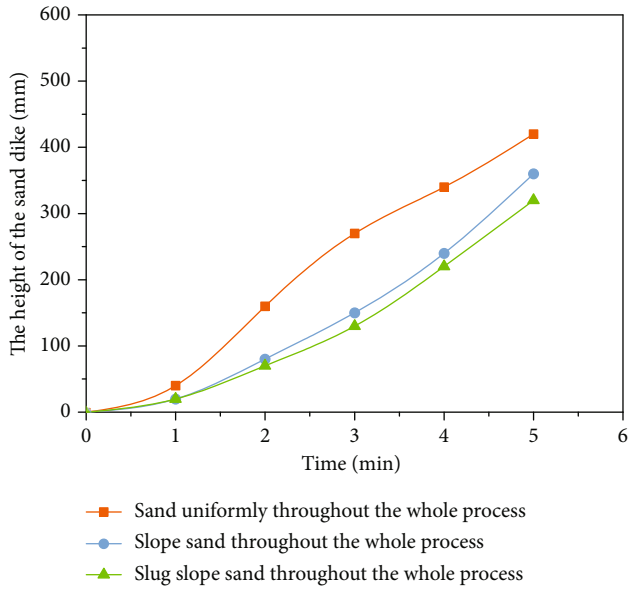

Figure 11: The height of the sand dike in sand carrying by slickwater with different proppant pumping schedules.

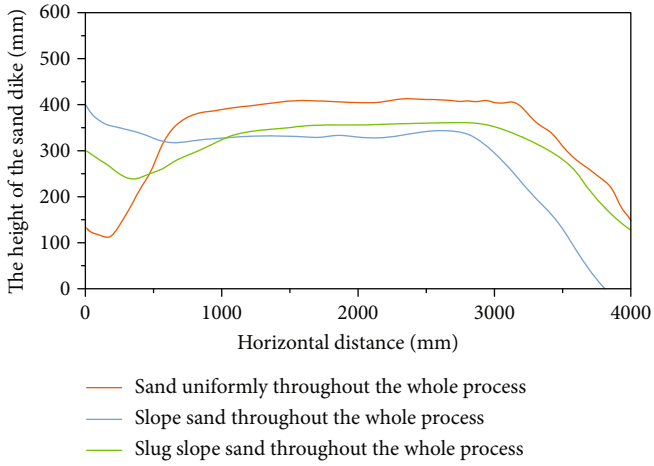

Figure 12: The shape of the sand dike formed by proppant sedimentation in sand carrying by slickwater with different proppant pumping schedules.

fracture inlet, which can form a proppant-supported fracture with high conductivity. Compared to slope sand addition, when slug slope sand addition is used, the proppant-free liquid has a more substantial scouring effect on the sand dike. It can transport the proppant to the depth of the fracture, thus forming a better proppant-supported fracture both near the fracture inlet and deeper in the fracture.

5. Conclusion

(1) With the pumping rate increases, the horizontal transport velocity of particles increases and the equilibrium height of the sand dike decreases, among which the equilibrium height of the sand dike is 0.44 m, 0.42 m, and 0.39 m for the pumping rate of 40 L/min, 60 L/min, and 80 L/min, respectively. The pumping rate increases cause the sand dike to become gentle and tend to transport deep into the fracture. Thus, the pumping rate should be increased as much as possible during the field operation process of volume fracturing

(2) When the viscosity is low viscous slickwater (3 mPa·s) and medium viscous slickwater (30 mPa·s), the equilibrium height of the sand dike produced is 0.41 m and 0.32 mm, respectively. Due to the high viscous slickwater (viscosity 100 mPa·s) with great sand-carrying capacity, the proppant advances evenly forward in the fracture, the settlement rate is slow, and the sand dike advances evenly in the fracture. During the field operation process, to form the proppant-supported fracture with a longer length and higher conductivity, slickwater with high viscosity should be selected as much as possible under the acceptable condition of reservoir damage, which can make the proppant deliver to the depth of fractures

(3) As the density of the proppant decreases, the equilibrium height of the sand dike decreases, where the equilibrium height of the sand dike is 0.45 m, 0.43 m, and 0.42 m when the density of the proppant is 1.80 g/cm^3, 1.65 g/cm^3, and 1.50 g/cm^3, and the sand dike thus becomes more gentle. During the field operation process, to form the proppant-supported fracture with a longer length and higher conductivity, low-density proppant should be used as much as possible under the condition that the compressive strength of the proppant is satisfied, which can enable the proppant to be delivered deeper into the fractures

(4) In different proppant pumping schedules, the sand dike height grows more rapidly when the whole process of uniform sand addition is used. Because the low concentration of proppant is selected at the beginning of the pumping schedule, the initial increase of the height of the sand dike is slower when slope sand addition is used. Furthermore, the concentration of proppant at the fracture inlet and the proppant-supported fracture with high conductivity during later in the pumping schedule. Compared with the slope sand addition, when slug slope sand addition is used, the proppant-free liquid has a stronger flushing effect on the sand dike. Thus, the proppant is transported to the depth of the fracture. And the proppant-supported fracture with higher conductivity both near the fracture inlet and deep in the fracture is formed. It can help achieve better oil and gas production

Data Availability

The experiment data used to support the findings of this study are included within the article.

Conflicts of Interest

The authors declare that they have no conflicts of interest.

Acknowledgments

This study was financially supported by the Scientific Research and Technology Development Project of Southwest Oil and Gas Field Company, PetroChina (No. 20210302-05 and No. 20210305-22).

References

[1] A. S. Ramlan, R. M. Zin, N. F. A. Bakar, and N. H. Othman, "Recent progress on proppant laboratory testing method: characterisation, conductivity, transportation, and erosivity," *Journal of Petroleum Science and Engineering*, vol. 205, article 108871, 2021.

[2] J. M. Estrada and R. Bhamidimarri, "A review of the issues and treatment options for wastewater from shale gas extraction by hydraulic fracturing," *Fuel*, vol. 182, pp. 292–303, 2016.

[3] C. Jia, M. Zheng, and Y. Zhang, "Unconventional hydrocarbon resources in China and the prospect of exploration and development," *Petroleum Exploration and Development*, vol. 39, no. 2, pp. 139–146, 2012.

[4] M. Paterniti, D. Kundert, M. Ramurthy, and D. Craig, "Production review of current stimulation techniques in the Jonah field," in *Paper Presented at the SPE Hydraulic Fracturing Technology Conference*, pp. 1–11, The Woodlands, TX, USA, February 2013.

[5] Y. Peng, J. Zhao, K. Sepehrnoori, Y. Li, and Z. Li, "The influences of stress level, temperature, and water content on the fitted fractional orders of geomaterials," *Mechanics of Time-Dependent Materials*, vol. 24, no. 2, pp. 221–232, 2020.

[6] Y. Peng, Y. Li, and J. Zhao, "A novel approach to simulate the stress and displacement fields induced by hydraulic fractures under arbitrarily distributed inner pressure," *Journal of Natural Gas Science & Engineering*, vol. 35, pp. 1079–1087, 2016.

[7] Y. Jinzhou Zhao, Y. L. Peng, and W. Xiao, "Analytical model for simulating and analyzing the influence of interfacial slip on fracture height propagation in shale gas layers," *Environmental Earth Sciences*, vol. 73, no. 10, pp. 5867–5875, 2015.

[8] Y. Peng, K. Jinzhou Zhao, Z. L. Sepehrnoori, and X. Feng, "Study of delayed creep fracture initiation and propagation based on semi- analytical fractional model," *Applied Mathematical Modelling*, vol. 72, pp. 700–715, 2019.

[9] Y. Jinzhou Zhao, Y. L. Peng, and Z. Tian, "Applicable conditions and analytical corrections of plane strain assumption in the simulation of hydraulic fracturing," *Petroleum Exploration and Development*, vol. 44, no. 3, pp. 454–461, 2017.

[10] Y. Peng, J. Zhao, K. Sepehrnoori, and Z. Li, "Fractional model for simulating the viscoelastic behavior of artificial fracture in shale gas," *Engineering Fracture Mechanics*, vol. 228, article 106892, 2020.

[11] H. Peng, F. Yu, J. Peng et al., "Research and application of a proppant transport experimental device for complex fractures in the unconventional reservoir," *Geofluids*, vol. 2022, Article ID 8356470, 10 pages, 2022.

[12] Y. Huan Peng, J. P. Fan, X. Gao, X. Gou, and Y. Yin, "Experimental evaluation and application of new size proppant for unconventional reservoir fracturing," *Fresenius Environmental Bulletin*, vol. 31, no. 3, pp. 2898–2907, 2022.

[13] H. Peng, J. Yang, J. Peng, H. Han, X. Gou, and Y. Jia, "Source analysis and countermeasure research of sand production after hydraulic fracturing in tight sandstone gas reservoir," *Lithosphere*, vol. 2022, no. Special 12, article 8342062, 2022.

[14] H. Bai, F. Zhou, M. Zhang et al., "Optimization and friction reduction study of a new type of viscoelastic slickwater system," *Journal of Molecular Liquids*, vol. 344, article 117876, 2021.

[15] N. K. Korlepara, K. Gore, and S. D. Kulkarni, "Understanding effect of fluid salinity on polymeric drag reduction in turbulent flows of slickwater fluids," *Journal of Petroleum Science and Engineering*, vol. 216, article 110747, 2022.

[16] S. Shi, J. Sun, K. Lv et al., "Comparative studies on thickeners as hydraulic fracturing fluids: suspension versus powder," *Gels*, vol. 8, no. 11, p. 722, 2022.

[17] A. V. Shibaev, A. A. Osiptsov, and O. E. Philippova, "Novel trends in the development of surfactant-based hydraulic fracturing fluids: a review," *Gels*, vol. 7, no. 4, p. 258, 2021.

[18] H. Peng, L. Zhou, J. Yang et al., "Influence of supercritical CO_2 on the formation sensitivity of tight sandstone," *Frontiers in Energy Research*, vol. 10, article 922941, 2022.

[19] H. Peng, J. Yang, J. Peng et al., "Experimental investigation of the mechanism of supercritical CO_2 interaction with tight sandstone," *Frontiers in Energy Research*, vol. 10, article 984144, 2022.

[20] S. Tong and K. K. Mohanty, "Proppant transport study in fractures with intersections," *Fuel*, vol. 181, no. 1, pp. 463–477, 2016.

[21] M. E. Fernández, M. Sánchez, and L. A. Pugnaloni, "Proppant transport in a scaled vertical planar fracture: vorticity and dune placement," *Journal of Petroleum Science and Engineering*, vol. 173, pp. 1382–1389, 2019.

[22] K. Shrivastava and M. M. Sharma, "Proppant transport in complex fracture networks," in *SPE Hydraulic Fracturing Technology Conference and Exhibition*, pp. 1–10, The Woodlands, TX, USA, 2018.

[23] R. Sahai, J. L. Miskimins, and K. E. Olson, "Laboratory results of proppant transport in complex fracture systems," in *SPE Hydraulic Fracturing Technology Conference*, pp. 1–26, The Woodlands, TX, USA, 2014.

[24] X. Liu, X. Zhang, Q. Wen, S. Zhang, Q. Liu, and J. Zhao, "Experimental research on the proppant transport behavior in nonviscous and viscous fluids," *Energy & Fuels*, vol. 34, no. 12, pp. 15969–15982, 2020.

[25] C.-H. Wu and M. M. Sharma, "Effect of perforation geometry and orientation on proppant placement in perforation clusters in a horizontal well," in *SPE Hydraulic Fracturing Technology Conference*, pp. 1–23, The Woodlands, TX, USA, 2016.

[26] H. Xiaodong, W. Kan, G. Li, J. Tang, and Z. Shen, "Effect of proppant addition schedule on the proppant distribution in a straight fracture for Slickwater treatment," *Journal of Petroleum Science and Engineering*, vol. 167, pp. 110–119, 2018.

[27] A. K. Olaleye, O. Shardt, G. Walker, H. E. A. Van den Akker, and H. E. A. Van den Akker, "Pneumatic conveying of cohesive dairy powder: experiments and CFD-DEM simulations," *Powder Technology*, vol. 357, pp. 193–213, 2019.

[28] S. Akhshik and M. Rajabi, "Simulation of proppant transport at intersection of hydraulic fracture and natural fracture of wellbores using CFD-DEM," *Particuology*, vol. 63, pp. 112–124, 2022.

[29] Y. Suri, S. Z. Islam, and M. Hossain, "Proppant transport in dynamically propagating hydraulic fractures using CFD-XFEM approach," *International Journal of Rock Mechanics and Mining Sciences*, vol. 131, article 104356, 2020.

[30] T. K. Guo, Z. Luo, J. Zhou et al., "Numerical simulation on proppant migration and placement within the rough and complex fractures," *Petroleum Science*, vol. 19, no. 5, pp. 2268–2283, 2022.

[31] G. Zhang, M. Li, and M. Gutierrez, "Simulation of the transport and placement of multi-sized proppant in hydraulic fractures using a coupled CFD-DEM approach," *Advanced Powder Technology*, vol. 28, no. 7, pp. 1704–1718, 2017.

[32] M. Baldini, C. M. Carlevaro, L. A. Pugnaloni, and M. Sánchez, "Numerical simulation of proppant transport in a planar fracture. A study of perforation placement and injection strategy," *International Journal of Multiphase Flow*, vol. 109, pp. 207–218, 2018.

[33] S. E. Gorucu, V. Shrivastava, and L. X. Nghiem, "Numerical simulation of proppant transport in hydraulically fractured reservoirs," in *SPE Reservoir Simulation Conference*, pp. 1–15, 2021.

[34] R. Sahai and R. G. Moghanloo, "Proppant transport in complex fracture networks - a review," *Journal of Petroleum Science and Engineering*, vol. 182, article 106199, 2019.

[35] X. Zhang, L. Yang, D. Weng, Z. Wang, and R. G. Jeffrey, "Numerical study on proppant transport in hydraulic fractures using a pseudo-3D model for multilayered Reservoirs," *SPE Journal*, vol. 27, no. 1, pp. 77–92, 2022.

[36] A. Isah, M. Hiba, K. Al-Azani, M. S. Aljawad, and M. Mahmoud, "A comprehensive review of proppant transport in fractured reservoirs: experimental, numerical, and field aspects," *Journal of Natural Gas Science and Engineering*, vol. 88, article 103832, 2021.

[37] A. Bello, J. Ozoani, and D. Kuriashov, "Proppant transport in hydraulic fractures by creating a capillary suspension," *Journal of Petroleum Science and Engineering*, vol. 208, article 109508, 2022.

[38] S. Yatin, S. Z. Islam, and M. Hossain, "Effect of fracture roughness on the hydrodynamics of proppant transport in hydraulic fractures," *Journal of Natural Gas Science and Engineering*, vol. 80, article 103401, 2020.

[39] E. Rivas and R. Gracie, "A monolithic coupled hydraulic fracture model with proppant transport," *Computer Methods in Applied Mechanics and Engineering*, vol. 372, article 113361, 2020.

[40] A. M. Skopintsev, E. V. Dontsov, P. V. Kovtunenko, A. N. Baykin, and S. V. Golovin, "The coupling of an enhanced pseudo-3D model for hydraulic fracturing with a proppant transport model," *Engineering Fracture Mechanics*, vol. 236, article 107177, 2020.